A single negative charge within the pore region of a cGMP-gated channel controls rectification, Ca^{2+} blockage, and ionic selectivity

(photoreceptors/ion channel/permeability)

ELISABETH EISMANN*, FRANK MÜLLER*, STEFAN H. HEINEMANN†, AND U. BENJAMIN KAUPP*

*Institut für Biologische Informationsverarbeitung, Forschungszentrum Jülich, Postfach 19 13, D-52425 Jülich, Germany; and †Max-Planck-Institut für Biophysikalische Chemie, Abteilung Membranbiophysik, Am Fassberg, D-37077 Göttingen, Germany

ABSTRACT Ca^{2+} ions control the cGMP-gated channel of rod photoreceptor cells from the external and internal face. We studied ion selectivity and blockage by Ca^{2+} of wild-type and mutant channels in a heterologous expression system. External Ca^{2+} blocks the inward current at micromolar concentrations in a highly voltage-dependent manner. The blockage at negative membrane voltages shows a steep concentration dependence with a Hill coefficient of ≈ 2. The blockage from the internal face requires ≈ 1000-fold higher Ca^{2+} concentrations. Neutralization of a glutamate residue (E363) in the putative pore region between transmembrane segments H4 and H5 induces outward rectification and changes relative ion conductances but leaves relative ion permeabilities nearly unaffected. The current blockage at -80 mV requires ≈ 2000-fold higher external Ca^{2+} concentrations and the voltage dependence is almost abolished. These results demonstrate that E363 represents a binding site for monovalent and divalent cations and resides in the pore lumen.

The cyclic nucleotide-gated channel of vertebrate rod photoreceptor cells (rod channel) belongs to a class of ligand-gated channels that are directly and cooperatively opened by the binding of cyclic nucleotides (cGMP or cAMP) (1–11). The rod channel is cation selective but does not appreciably discriminate between monovalent alkali cations (1, 4, 12–17). Divalent cations also permeate the rod channel and thereby block the Na^+ current in a voltage-dependent manner (15–29). Ca^{2+} entry is of great physiologic importance because Ca^{2+} is part of a negative feedback mechanism that regulates the recovery of the light response and light adaptation (for review, see refs. 30 and 31). Blockage by both external and internal Ca^{2+} is voltage dependent, indicating a binding site(s) for Ca^{2+} within the channel pore (26, 28). Internal Ca^{2+} decreases both the open probability and the single-channel conductance (32). External Ca^{2+} appears to reduce single-channel conductance from 25 to ≈ 0.1 pS (33, 34).

Comparison with the protein sequences of K^+ channels has led to the prediction that the pore region of the rod channel is located between transmembrane segments H4 and H5 (refs. 7, 8, and 35–37; for reviews, see refs. 38–41). The pore region of K^+ channels contains two adjacent amino acid residues (Y445, G446; Fig. 1) that are missing in the respective region of the rod channel. By deletion of these residues, the Shaker K^+ channel is converted into a nonselective cation channel (36). The sensitivity to blockage by divalent cations that is increased in the deletion mutant is controlled by the adjacent acidic residue D447 (36). This residue corresponds to glutamate-363 (E363) in the pore region of the rod channel. We demonstrate by heterologous expression of wild-type (wt) and mutant rod channels that E363 is crucial for binding

of both monovalent and divalent cations and resides inside the pore lumen.

MATERIALS AND METHODS

Site-Directed Mutagenesis and in Vitro Transcription. The point mutations K346Q, E363Q, R369Q, and E372Q in the rod channel polypeptide were introduced by polymerase chain reaction using the protocol of ref. 43. All mutations were verified by sequencing of the inserted fragment (44). mRNAs specific for wt and mutant channels were synthesized in vitro (45). Synthesis was primed with m7G(5′)ppp(5′)G.

Functional Expression. Channel properties were studied with the patch-clamp technique in inside-out and outside-out patches after expression in Xenopus oocytes (46–49). Relative ion permeabilities were determined from the reversal potential (V_{rev}) of inside-out patches under symmetrical bi-ionic conditions. Pipette and bath solutions contained 100 mM KCl, 20 mM Tris·HCl, and 2 mM EGTA (pH 7.4). KCl in the perfusion medium was replaced by an equimolar concentration of another monovalent cation. Currents were activated by 1 mM cGMP. Leak currents measured without cGMP were subtracted from each trace. For the measurement of the current blockage by Ca^{2+}, the pipette and bath solutions contained 100 mM K^+-gluconate, 5 mM KCl, 10 mM Hepes adjusted with 10 mM Tris to pH 7.4. Ca^{2+}-gluconate (0.1–25 mM) was added to the solutions superfusing the cytoplasmic side. Leak currents were recorded in the presence of the respective Ca^{2+} concentration but without cGMP. In the outside-out configuration, the pipette solution contained 115 mM NaCl or KCl, 1.8 mM EGTA, 10 mM Hepes·NaOH (pH 7.2), and 1 mM cGMP. The bath solution contained 115 mM NaCl and 10 mM Hepes·NaOH (pH 7.2). Ca^{2+} and Mg^{2+} were added as chloride salts to the superfusing solutions. Low Ca^{2+} and Mg^{2+} concentrations were adjusted by EGTA or nitrilotriacetic acid and by EDTA or N-hydroxyethylethylenediaminetriacetic acid, respectively (50). Only outside-out patches with negligible leak current were considered for analysis (see Fig. 4C, dashed line).

RESULTS

Ion Selectivity of wt Channel. The ion selectivity of the heterologously expressed rod channel was determined from relative ion permeabilities by measuring reversal potentials V_{rev} and from current ratios at $V_m = +50$ mV. Fig. 2A shows a series of current–voltage (I/V) recordings from inside-out patches at saturating cGMP concentrations. As has been reported (1, 4, 12–17), the channel does not discriminate well between alkali ions (Table 1). Ion permeabilities of the bovine rod channel measured in situ (14) and in the oocyte system (see also ref. 4) were largely similar except for Li^+. In excised membrane patches of the bovine or amphibian rod, Li^+ is

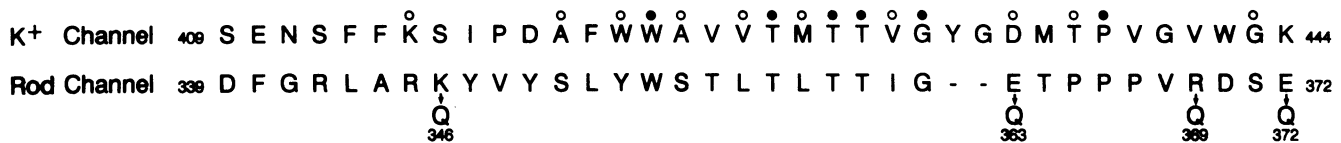Abbreviation: wt, wild type.

K⁺ Channel 409 S E N S F F K̊ S I P D Å F W W Å V V T M T T V G Y G D M T P V G V W G̊ K 444

Rod Channel 339 D F G R L A R K Y V Y S L Y W S T L T L T T I G - - E T P P P V R D S E 372
                                   ↕   ↕   ↕   ↕
                                   Q   Q   Q   Q
                                  346   363   369   372

FIG. 1.   Amino acid sequences of the putative pore region of a Shaker K⁺ channel (42) and the rod channel (4); amino acid residues are given in one-letter code; solid and open circles represent identical and conserved residues, respectively; mutated amino acids are indicated.

more permeant than Na⁺ or K⁺ (12–14). The rod channel expressed in oocytes exists as a homooligomer, whereas *in situ* it is composed of at least two genetically distinct subunits (51). This fact may account for the observed differences.

A qualitatively similar selectivity series is calculated from the conductance ratios (Table 1). However, currents carried by Li⁺ and Cs⁺ are much smaller than expected from the relative ion permeabilities, both in the native membrane (14) and in oocytes (Fig. 2A).

Ion Selectivity of Mutant Channels. When E363 was replaced by glutamine (E363Q) the channel properties changed dramatically. First, I/V curves became strongly outward rectifying (Fig. 2B). Second, I/V curves for all alkali ions became similar. This similarity is even more pronounced when the currents are compared at the same driving force by shifting the I/V curves on the voltage axis by $-V_{rev}$ (Fig. 2B *Inset*; Table 1). In contrast, relative ion permeabilities were much less affected (Table 1), except for subtle changes in the case of Li⁺ and Rb⁺ ions.

These changes in the mutant E363Q are position specific and do not result from unintended structural perturbations that propagate through the entire pore region. Neutralization of other charged residues in the neighborhood of E363 (K346Q, R369Q, E372Q; see Fig. 1) did not change channel properties significantly (Table 1).

Blockage by Internal Ca²⁺. Millimolar concentrations of Ca²⁺ ions reduced both inward and outward K⁺ currents in a voltage-dependent manner (Fig. 3A). The fraction of unblocked current (I_{Ca}/I) was diminished by depolarization (Fig. 3A *Inset*). Such behavior is typical of a blocking ion that binds within the pore, with penetration facilitated by depolarization. At moderate Ca²⁺ concentrations (0.5–1 mM) the blockage is partially relieved at positive V_m, probably due to permeation of Ca²⁺ through the pore. Constants K_i of half-

maximal current inhibition and Hill coefficients were determined by a least-squares fit procedure using the Hill equation (Table 2).

In mutant E363Q, the ability of Ca²⁺ to block monovalent current was reduced ≈3-fold, and the blockage depended considerably less on V_m (Fig. 3B and *Inset*). In mutant E372Q, the voltage dependence and the K_i constant of Ca²⁺ blockage was not significantly different from that of the wt channel (1.2 mM at +80 mV; 5.3 mM at −80 mV).

Blockage by External Ca²⁺. Ca²⁺ ions blocked the rod channel from the extracellular side in a highly voltage-dependent fashion (Fig. 4A). At medium Ca²⁺ concentrations, the blockage increased when V_m was made less positive. It was maximal at a voltage $V_c \le -30$ mV and decreased again with further hyperpolarization (Fig. 4A *Inset*). At high Ca²⁺ concentrations (≥1 mM) the I_{Ca}/I ratio fell monotonically by making V_m more negative, and no sign of recovery even at −100 mV was observed (Fig. 4A *Inset*).

The channel blockage by external Mg²⁺ ions was qualitatively similar to the blockage by Ca²⁺. It was most pronounced at large negative V_m and diminished at increasingly positive V_m (Fig. 4B). However, blockage at all Mg²⁺ concentrations tested was not relieved at negative V_m (Fig. 4B *Inset*). This difference suggests that Mg²⁺ is less permeant than Ca²⁺, confirming results by others (24, 26).

The concentration dependence of the Ca²⁺ blockage was influenced by voltage. At positive V_m, the blockage can be described by binding of one Ca²⁺ ion to a single site ($K_i = 310$ μM; Hill coefficient, $n = 0.9$; Fig. 4D; Table 2). K_i decreased continuously by making V_m less positive until it reached a minimum at V_c ($K_i = 2.2$ μM) and increased again when V_m became more negative. The Hill coefficient was maximal at V_c ($n = 2.3$). The Hill coefficient for Mg²⁺ blockage at −80 mV ($n = 1.3$) was also significantly larger than at +80 mV (n
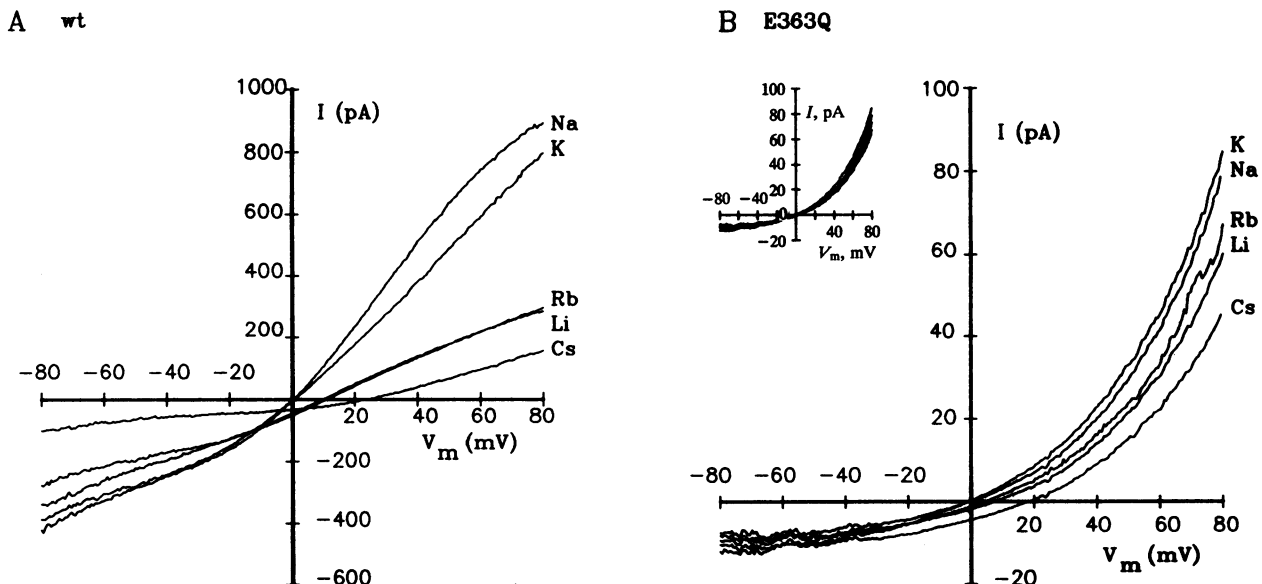

A wt

B E363Q

FIG. 2.   Ionic selectivity of rod wt and mutant channels. Current–voltage recordings obtained from voltage ramps in inside-out patches. (A) Rod wt channel. (B) Mutant E363Q. (*Inset*) Voltage ramps as in B were adjusted such that currents for each test ion reversed at 0 mV, yielding identical driving forces; same patch as in B.

Table 1. Relative ion permeability and conductance ratios of wt and mutant channels

	Permeability ratio $P(X)/P(K)$					Relative conductance $g(X)/g(K)$				
	K	Na	Rb	Li	Cs	K	Na	Rb	Li	Cs
Rod wt	1	0.84	0.7	0.56	0.44	1	1.18	0.43	0.38	0.26
K346Q	1	0.83	0.7	0.52	0.38	1	1.03	0.5	0.37	0.28
E363Q	1	0.79	0.85	0.68	0.45	1	0.92	0.92	0.87	0.86
R369Q	1	0.84	0.68	0.57	0.36	1	1.15	0.46	0.36	0.28
E372Q	1	0.82	0.71	0.53	0.43	1	0.87	0.42	0.3	0.25

Reversal potentials (V_{rev}) were measured under bi-ionic conditions with saturating concentrations of cGMP, averaged for 3–15 patches and corrected for liquid junction potentials. Number x of patches is given in brackets, V_{rev} is in mV, SD is in parentheses. Rod wt [x = 3]: K = 0, Na = 4.4 (0.29), Rb = 8.9 (0.82), Cs = 20.8 (1.82), Li = 14.8 (0.55). K346Q [x = 5]: K = 0, Na = 4.7 (0.47), Rb = 8.92 (0.97), Cs = 24.1 (1.84), Li = 16.38 (0.29). E363Q [x = 7]: K = 0, Na = 5.88 (0.82), Rb = 4.09 (1.29), Cs = 20.26 (3.53), Li = 9.63 (0.89). R369Q [x = 15]: K = 0, Na = 4.49 (0.26), Rb = 9.64 (0.85), Cs = 25.85 (3.47), Li = 14.36 (1.36). E372Q [x = 9]: K = 0, Na = 5.07 (0.26), Rb = 8.48 (0.97), Cs = 21.34 (2.76), Li = 15.96 (0.97). Permeability ratios were calculated from V_{rev} using the Goldman–Hodgkin–Katz equation. The conductance sequence was derived from currents at +50 mV corrected for V_{rev} to yield identical driving force for the different ions.

= 0.9). These results are consistent with the notion that two blocking ions bind to a high-affinity site in a cooperative fashion.

In mutant E363Q, the strong voltage-dependent blockage by micromolar Ca^{2+} concentrations at negative V_m was almost completely abolished (Fig. 4C and Inset). Approximately 2000-fold higher external Ca^{2+} concentrations were required to suppress the current by half (Fig. 4D; Table 2). The K_i values for the blockage at positive V_m were less affected. For both Ca^{2+} and Mg^{2+} ions, the blockage cannot be described by a simple binding scheme, because Hill coefficients decrease significantly below unity (n_{Ca} = 0.3–0.7; n_{Mg} = 0.4–0.6).

Location of the Blocking Site. We estimated the location of the blocking site from the voltage dependence of blockage by external Mg^{2+}. The fractional electric distance δ derived from the slope of the plot $\ln(I/I_{Mg} - 1)$ versus V_m equaled 0.35. This value implies that divalent cations entering the pore from the extracellular medium traverse 35% of the full transmembrane field to reach their binding site.

DISCUSSION

Our results identify a single negatively charged glutamate residue that controls ion entry and channel blockage. Replacement of this amino acid by a neutral residue affects ion permeabilities only marginally, whereas the relative ion conductances are changed drastically. In the wt channel the amplitudes of the outward currents strongly depend on the ion species at the cytoplasmic side, while in mutant E363Q outward currents carried by different ion species become very similar. This result suggests that E363 controls the rate at which different ions exit from the pore to the external medium. Although E363 may also influence the location of other amino acid residues within the aqueous pore and thereby may exert some minor effects on the relative ion permeability, mutant E363Q illustrates that ion permeability and conductance are controlled by different residues in the pore. Therefore, E363 probably does not constitute the "selectivity filter" at the narrowest part along the permeation pathway but instead might be crucial for binding ions at the entrance to the channel lumen. The strong outward rectification of current in mutant E363Q would be consistent with the alteration of an energy barrier at the external entrance. We cannot exclude changes in channel gating that may also contribute to the rectification.

The results identify distinct mechanisms of blockage by divalent cations. Internal Ca^{2+} or Mg^{2+} suppresses both inward and outward currents. The voltage-dependent fraction of this blockage disappears in the E363Q mutant, whereas a voltage-independent blockage persists. Blockage is also observed at large negative V_m in wt channel (see Fig. 2A), suggesting an additional binding site(s) at the cytosolic face of the channel protein that might control the open probability (26, 32). The pronounced voltage dependence of blockage by external divalent cations in the wt channel provides strong evidence that Ca^{2+} ions must enter the pore to reach the blocking site, which is located ≈35% of the fractional electrical distance from the external surface. External Ca^{2+} blockage can be relieved by either hyperpolarization or depolarization of the membrane; thus Ca^{2+} ions can exit the pore in either direction. Mg^{2+} blockage is relieved
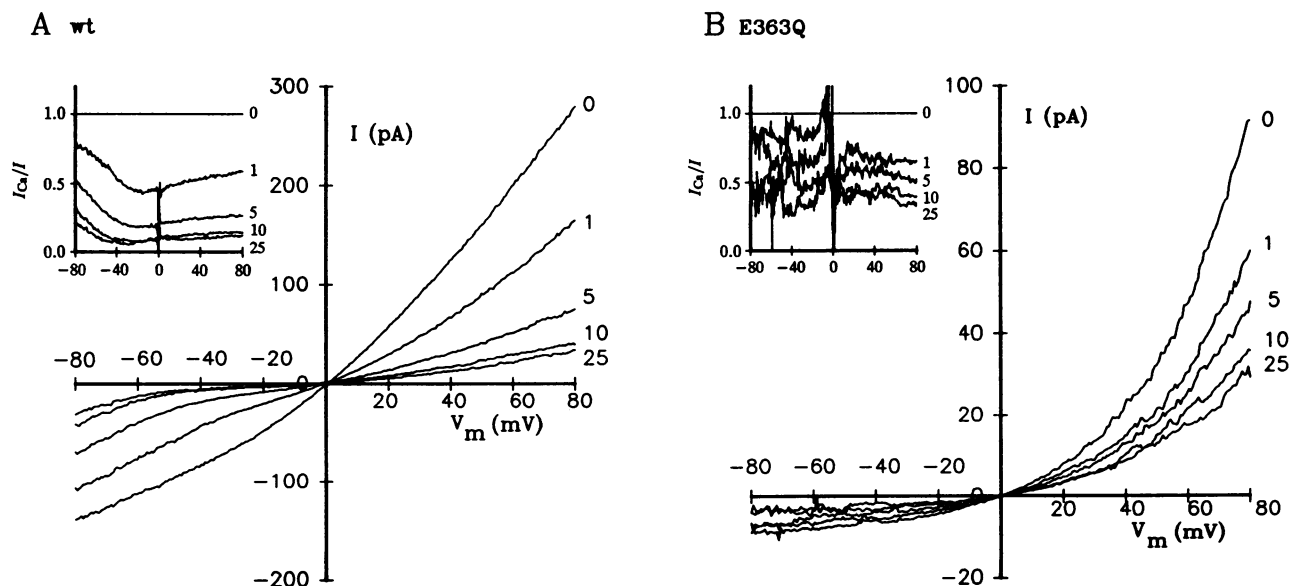
A wt

B E363Q

Fig. 3. Blockage of monovalent current by internal Ca^{2+} in inside-out patches. Numbers at each trace indicate the Ca^{2+} concentration (mM) at the internal face of the membrane. (Inset) Voltage dependence of the ratio of unblocked current I_{Ca}/I. (A) Rod wt channel. (B) Mutant E363Q.

Table 2. Inhibition constants K_i for Ca^{2+} and Mg^{2+} blockage

	Rod wt			E363Q*	
	+80 mV	−30 mV	−80 mV	+80 mV	−80 mV
Ca_i^{2+}	2.3 ± 0.5 mM (4)	ND	6.9 ± 1.9 mM (4)	8.9 ± 4.3 mM (2)	11.6 ± 3.7 mM (2)
	$n = 1.0 ± 0.15$	ND	$n = 1.0 ± 0.2$	$n = ≈0.4$	$n = 0.3–0.7$
Ca_o^{2+}	310 ± 100 μM (6)	2.2 ± 0.5 μM (6)	3.6 ± 0.5 μM (6)	25 ± 21 mM (5)	7 ± 8 mM (5)
	$n = 0.9 ± 0.2$	$n = 2.3 ± 0.4$	$n = 1.7 ± 0.4$	$n = 0.5 ± 0.1$	$n = 0.5 ± 0.2$
Mg_o^{2+}	1.9 ± 1.3 mM (3)	ND	15.3 ± 3.3 μM (3)	≥10 mM (3)	≈10 mM (3)
	$n = 0.9 ± 0.3$	ND	$n = 1.3 ± 0.1$		

Data are presented as means ± SD. Subscript i, inside; subscript o, outside; ND, not determined. Number of experiments is given in parentheses. K_i values for half-maximal inhibition were determined by a least-squares fit procedure using the Hill equation $I_D/I = 1 - C_D^n/(C_D^n + K_i^n)$. C_D denotes the concentration of divalent cations; n is the Hill coefficient.
*Divalent cation block was incomplete at the highest concentrations of divalent cations tested and was highly variable.

only if the inside of the cell is made positive. This behavior is expected if Mg^{2+} is less permeant than Ca^{2+} (24, 26). Blocking of the wt channel by external divalent cations at positive voltages can be described by binding to a single site, indicating that one ion suffices to occlude the ionic pathway. At negative voltages the channel becomes extremely sensitive to blockage by Ca^{2+} and the Hill coefficient for blocking is >1, suggesting that two or more ions are necessary to

occlude the pore. The channel is composed of several subunits (4) and a ring of carboxylate groups might form a high-affinity binding site(s) that can accommodate more than one Ca^{2+} ion at a time. Upon replacement of E363 by a neutral residue, the voltage-dependent Ca^{2+} or Mg^{2+} blockage is abolished. A similar result has been recently reported (52). The blockage that persists at high external Ca^{2+} concentrations may result from negative fixed charges in the
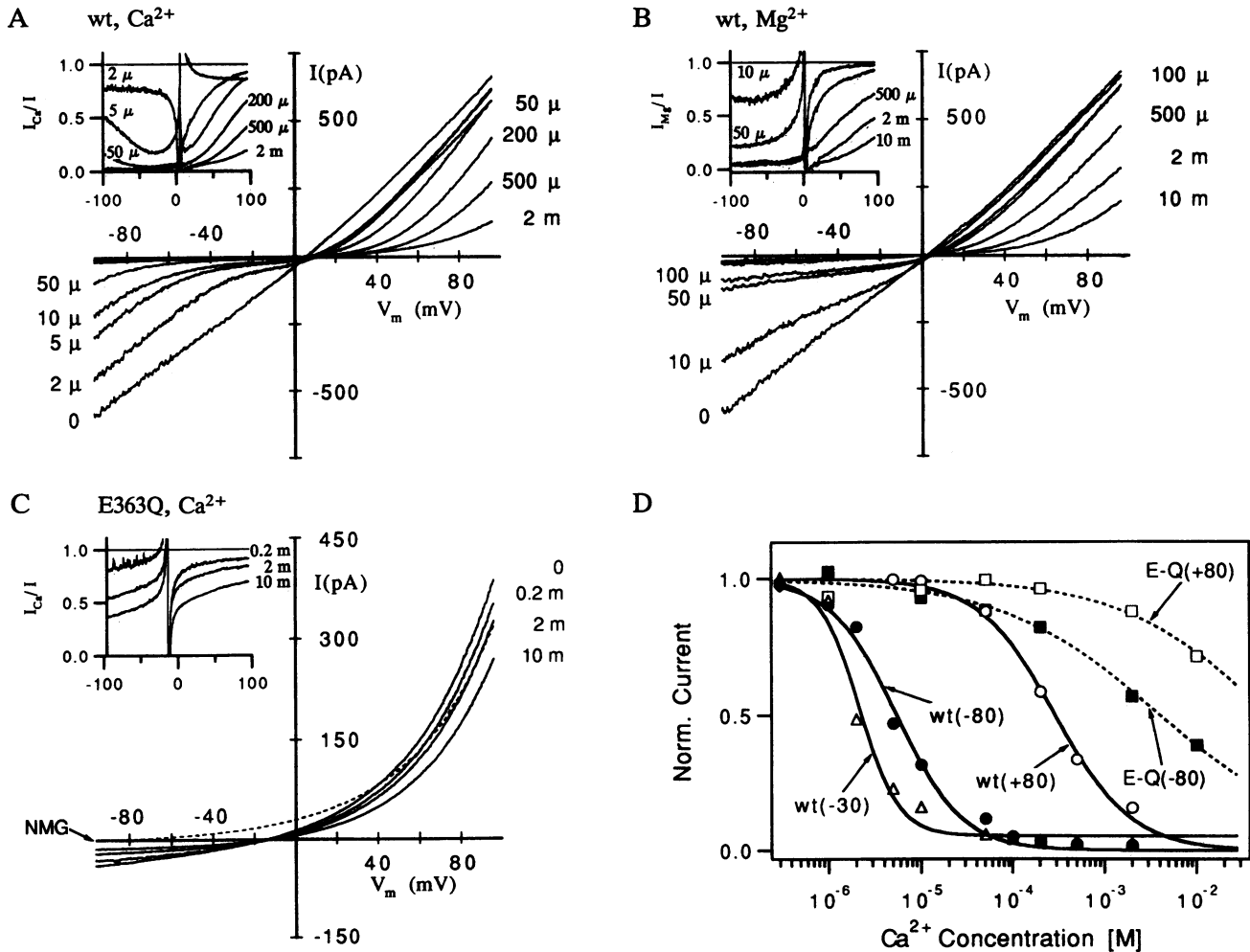

FIG. 4. Blockage of monovalent current by external Ca^{2+} and Mg^{2+} in outside-out patches. (A and B) Current–voltage recordings of the wt channel. (A) With increasing Ca^{2+} concentrations. (B) With increasing Mg^{2+} concentrations. Numbers at each trace indicate concentrations of divalent ions (μM or mM). (Insets) Voltage dependence of ratio of unblocked current (A, I_{Ca}/I; B, I_{Mg}/I). (C) Current–voltage recordings of mutant E363Q with increasing external Ca^{2+} concentrations. Dashed line represents current that remains when K^+ was replaced by the impermeable ion N-methylglucamine (NMG). This current was used to estimate inward leak current. (Inset) As in A. (D) Dose dependence of current blockage in wt at +80 mV (o), −30 mV (△), and −80 mV (●) and in mutant E363Q at +80 mV (□) and −80 mV (■). Smooth curves represent a least-squares fit of the equation $I_{Ca}/I = 1 - C_{Ca}^n/(C_{Ca}^n + K_i^n)$ to the experimental data. Rod wt, K_i (+80 mV) = 288 μM, $n = 1.0$; K_i (−80 mV) = 5.4 μM, $n = 1.2$; K_i (−30 mV) = 2.3 μM, $n = 2.1$. Mutant E363Q, K_i (+80 mV) = 60 mM, $n = 0.55$; K_i (−80 mV) = 4 mM, $n = 0.5$.

Neurobiology: Eismann *et al.*

Proc. Natl. Acad. Sci. USA 91 (1994)   1113

antechamber of the channel, which concentrate Ca^{2+} over Na^+ at the entrance of the pore.

The results are reminiscent of the permeation mechanism in Ca^{2+} channels (for review, see ref. 53). Ca^{2+} blocks monovalent current through these channels at micromolar concentrations. At higher concentrations, Ca^{2+} itself permeates and double occupancy of the pore is essential for high Ca^{2+} flux rates. While this hypothesis for rod channels needs to be substantiated by future work, our results suggest similar mechanisms of ion permeation in Ca^{2+}- and cyclic nucleotide-gated channels. A high-affinity binding site for Ca^{2+} ions that is formed by a ring of four conserved glutamate residues at positions equivalent to E363 of the rod channel has been recently identified in the pore of L-type Ca^{2+} channels (54).

1. Fesenko, E. E., Kolesnikov, S. S. & Lyubarsky, A. L. (1985) *Nature (London)* 313, 310–313.
2. Haynes, L. & Yau, K.-W. (1985) *Nature (London)* 317, 61–64.
3. Nakamura, T. & Gold, G. H. (1987) *Nature (London)* 325, 442–444.
4. Kaupp, U. B., Niidome, T., Tanabe, T., Terada, S., Bönigk, W., Stühmer, W., Cook, N. J., Kangawa, K., Matsuo, H., Hirose, T., Miyata, T. & Numa, S. (1989) *Nature (London)* 342, 762–766.
5. Ludwig, J., Margalit, T., Eismann, E., Lancet, D. & Kaupp, U. B. (1990) *FEBS Lett.* 270, 24–29.
6. Dhallan, R. S., Yau, K.-W., Schrader, K. A. & Reed, R. R. (1990) *Nature (London)* 347, 184–187.
7. Goulding, E. H., Ngai, J., Kramer, R. H., Colicos, S., Axel, R., Siegelbaum, S. A. & Chess, A. (1992) *Neuron* 8, 45–58.
8. Bönigk, W., Altenhofen, W., Müller, F., Dose, A., Illing, M., Molday, R. S. & Kaupp, U. B. (1993) *Neuron* 10, 865–877.
9. Yau, K.-W. & Baylor, D. A. (1989) *Annu. Rev. Neurosci.* 12, 289–327.
10. Kaupp, U. B. (1991) *Trends Neurosci.* 14, 150–157.
11. Kaupp, U. B. & Altenhofen, W. (1992) in *Sensory Transduction*, ed. Corey, D. (Rockefeller Univ. Press, New York), pp. 133–150.
12. Furman, R. E. & Tanaka, J. C. (1990) *J. Gen. Physiol.* 96, 57–82.
13. Menini, A. (1990) *J. Physiol. (London)* 424, 167–185.
14. Lühring, H., Hanke, W., Simmoteit, R. & Kaupp, U. B. (1990) in *Sensory Transduction*, eds. Borsellino, A., Cervetto, L. & Torre, V. (Plenum, New York), pp. 169–173.
15. Hodgkin, A. L., McNaughton, P. A., Nunn, B. J. & Yau, K.-W. (1984) *J. Physiol. (London)* 350, 649–680.
16. Yau, K.-W. & Nakatani, K. (1984) *Nature (London)* 309, 352–354.
17. Hodgkin, A. L., McNaughton, P. A. & Nunn, B. J. (1985) *J. Physiol. (London)* 358, 447–468.
18. Stern, J. H., Kaupp, U. B. & MacLeish, P. R. (1986) *Proc. Natl. Acad. Sci. USA* 83, 1163–1167.
19. Haynes, L. W., Kay, A. R. & Yau, K.-W. (1986) *Nature (London)* 321, 66–70.
20. Zimmerman, A. L. & Baylor, D. A. (1986) *Nature (London)* 321, 70–72.
21. Stern, J. H., Knutsson, H. & MacLeish, P. R. (1987) *Science* 236, 1674–1678.
22. Menini, A., Rispoli, G. & Torre, V. (1988) *J. Physiol. (London)* 402, 279–300.
23. Lamb, T. D. & Matthews, H. R. (1988) *J. Physiol. (London)* 403, 473–494.
24. Nakatani, K. & Yau, K.-W. (1988) *J. Physiol. (London)* 395, 695–729.
25. Ildefonse, M. & Bennett, N. (1991) *J. Membr. Biol.* 123, 133–147.
26. Colamartino, G., Menini, A. & Torre, V. (1991) *J. Physiol. (London)* 440, 189–206.
27. Zimmerman, A. L. & Baylor, D. A. (1992) *J. Physiol. (London)* 449, 759–783.
28. Karpen, J. W., Brown, R. L., Stryer, L. & Baylor, D. A. (1993) *J. Gen. Physiol.* 101, 1–25.
29. Tanaka, J. C. & Furman, R. E. (1993) *J. Membr. Biol.* 131, 245–256.
30. Pugh, E. N. & Lamb, T. D. (1990) *Vision Res.* 30, 1923–1948.
31. Kaupp, U. B. & Koch, K.-W. (1992) *Annu. Rev. Physiol.* 54, 153–175.
32. Sesti, F., Straforini, M., Lamb, T. D. & Torre, V. (1993) *J. Physiol. (London)*, in press.
33. Bodoia, R. D. & Detweiler, P. B. (1985) *J. Physiol. (London)* 367, 183–216.
34. Gray, P. & Attwell, D. (1985) *Proc. R. Soc. London B* 223, 379–388.
35. Guy, H. R., Durell, S. R., Warmke, J., Drysdale, R. & Ganetzky, B. (1991) *Science* 254, 730.
36. Heginbotham, L., Abramson, T. & MacKinnon, R. (1992) *Science* 258, 1152–1155.
37. Goulding, E. H., Tibbs, G. R., Liu, D. & Siegelbaum, S. A. (1993) *Nature (London)* 364, 61–64.
38. Stühmer, W. (1991) *Annu. Rev. Biophys. Biophys. Chem.* 20, 65–78.
39. Pongs, O. (1992) *Trends Pharmacol. Sci.* 13, 359–365.
40. Miller, C. (1992) *Curr. Biol.* 2, 573–575.
41. Jan, L. Y. & Jan, Y. N. (1992) *Annu. Rev. Physiol.* 54, 537–555.
42. Pongs, O., Kecskemethy, N., Müller, R., Krah-Jentgens, I., Baumann, A., Kiltz, H. H., Canal, I., Llamazares, S. & Ferrus, A. (1988) *EMBO J.* 7, 1087–1096.
43. Herlitze, S. & Koenen, M. (1990) *Gene* 91, 143–147.
44. Sanger, F., Nicklen, S. & Coulson, A. R. (1977) *Proc. Natl. Acad. Sci. USA* 74, 5463–5467.
45. Melton, D. A., Krieg, P. A., Rebagliati, M. R., Maniatis, T., Zinn, K. & Green, M. R. (1984) *Nucleic Acids Res.* 12, 7035–7056.
46. Hamill, O. P., Marty, A., Neher, E., Sakmann, B. & Sigworth, F. J. (1981) *Pflügers Arch.* 391, 85–100.
47. Stühmer, W., Methfessel, C., Sakmann, B., Noda, M. & Numa, S. (1987) *Eur. Biophys. J.* 14, 131–138.
48. Methfessel, C., Witzemann, V., Takahashi, T., Mishina, M., Numa, S. & Sakmann, B. (1986) *Pflügers Arch.* 407, 577–588.
49. Altenhofen, W., Ludwig, J., Eismann, E., Kraus, W., Bönigk, W. & Kaupp, U. B. (1991) *Proc. Natl. Acad. Sci. USA* 88, 9868–9872.
50. Heinemann, S. H., Terlau, H., Stühmer, W., Imoto, K. & Numa, S. (1992) *Nature (London)* 356, 441–443.
51. Chen, T. Y., Peng, Y. W., Dhallan, R. S., Ahamed, B., Reed, R. R. & Yau, K.-W. (1993) *Nature (London)* 362, 764–767.
52. Root, M. J. & MacKinnon, R. (1993) *Neuron* 11, 459–466.
53. Tsien, R. W., Hess, P., McCleskey, E. W. & Rosenberg, R. L. (1987) *Annu. Rev. Biophys. Biophys. Chem.* 16, 265–290.
54. Yang, J., Ellinor, P. T., Sather, W. A., Zhang, J.-F. & Tsien, R. W. (1993) *Nature (London)* 366, 158–161.